

## Initialization of Seasonal Forecasts Assimilating Sea Level and Temperature Observations

J. SEGSCHEIDER,\* D. L. T. ANDERSON, J. VIALARD, M. BALMASEDA, AND T. N. STOCKDALE

*European Centre for Medium-Range Weather Forecasts, Reading, Berkshire, United Kingdom*

A. TROCCOLI,<sup>+</sup> AND K. HAINES<sup>#</sup>

*Meteorology Department, University of Edinburgh, Edinburgh, United Kingdom*

(Manuscript received 27 December 2000, in final form 29 May 2001)

### ABSTRACT

In this paper, the combined assimilation of satellite observed sea level anomalies and in situ temperature data into a global ocean model, which is used to initialize a coupled ocean–atmosphere forecast system, is described. The altimeter data are first used to create synthetic temperature observations, which are then combined with the directly observed temperature profiles in an optimum interpolation scheme. In addition to temperature, salinity is corrected based on a preservation of the model's local temperature–salinity relationship. Coupled forecasts with a lead time of up to 6 months are initialized from the ocean analyses and the impact of the data assimilation on both the ocean analysis and the coupled forecasts is investigated. It is shown that forecasts of sea surface temperature anomalies in the Niño-3 area can be improved by initializing the coupled forecast model with the ocean analysis in which temperature and altimeter data are assimilated in combination. The results further imply that a good simulation of the salinity field is required to make optimum use of the altimeter data.

### 1. Introduction

The El Niño–Southern Oscillation (ENSO) phenomenon can now be simulated reasonably well with coupled ocean–atmosphere models and attempts to predict the behavior of the coupled system over timescales of several months are now made regularly at a number of institutes. As the atmosphere on synoptic scales behaves in a chaotic manner beyond timescales of a few days, it is mainly the ocean that carries the potential for predictive skill (Palmer and Anderson 1994). In particular, equatorial waves such as the eastward-propagating Kelvin waves and the westward off-equatorial Rossby waves are thought to carry the memory on which forecasts are based and are important components of the so-called delayed-action oscillator (Schopf and Suarez

1988). Although the delayed-action idea is appealing for understanding how predictability might arise, it has proved to be of little practical use in terms of making predictions. Fully dynamical coupled ocean–atmosphere models offer the most comprehensive approach to ENSO forecasting.

Such models require an accurate description of the ocean state as initial conditions for such a forecast. Observations of the ocean are too sparse to allow the derivation of an accurate analysis based on observations alone, however. Rather an estimate of the ocean state is obtained by combining the observations with the results from the dynamical ocean model through data assimilation. This is usually done by using a sequential approach: the model is run for a certain time, the observations are gathered, and an analysis is performed by combining the model first guess with the new observations. After that, the model is run for the next interval. The ocean models that are used to yield initial conditions for the coupled forecast system are not perfect, however, and neither are the forcing fields of momentum, heat, and freshwater that are used to integrate the model forward in time. Data assimilation is used to correct for these errors.

The ocean analyses have used observations mainly of sea surface temperature (SST), subsurface temperatures ( $T_{\text{sub}}$ ), and, more recently, sea level anomalies (Ji et al. 2000; Carton et al. 1996, 2000; Segsneider et

\* Current affiliation: Istituto Nazionale di Geofisica e Vulcanologia, Rome, Italy.

<sup>+</sup> Current affiliation: National Aeronautics and Space Administration Goddard Earth Sciences and Technology, NASA Seasonal to Interannual Prediction Project, Greenbelt, Maryland.

<sup>#</sup> Current affiliation: Environmental Systems Science Centre, University of Reading, Reading, Berkshire, United Kingdom.

*Corresponding author address:* Dr. J. Segsneider, Istituto Nazionale di Geofisica e Vulcanologia, ISAO-CNR, via P. Gobetti 101, 40129 Bologna, Italy.  
E-mail: Segsneider@ingv.it

al. 2000a, hereafter SEG2000a). SST is observed sufficiently densely from satellite and ships to allow an analysis without a model (Reynolds and Smith 1995) and this SST field can then be strongly nudged into the ocean model. Subsurface temperatures are less frequently observed and are generally assimilated via optimum interpolation (OI; Derber and Rosati 1989; Smith et al. 1991; and Daley 1991 for a more general description of OI). The application of more sophisticated assimilation schemes than a sequential OI; namely, the Ensemble Kalman Filter (EnKF) and 4D-Var, in quasi-operational global models is an ongoing research issue, but so far only test studies using subsurface temperature observations have been performed (Weaver and Vialard 1999). The use of altimetry in EnKF and 4D-Var assimilation schemes is at an even earlier stage and will most likely take another couple of years to be developed to a level suitable for near-real-time use.

To make use of both the direct observations of  $T_{\text{sub}}$  and the better coverage provided by altimeter observations, the combined assimilation of  $T_{\text{sub}}$  and sea level anomalies (SLAs) is required. SLAs are currently assimilated either by projecting the surface signal to the subsurface by use of statistical relationships between SLAs and subsurface temperature (e.g., Mellor and Ezer 1991; Carton et al. 1996; Fischer et al. 1997; Vossepoel et al. 1999; Ji et al. 2000) or by vertical shifts of the model's local temperature and salinity profiles in order to match the observed sea level based on the work of Cooper and Haines (1996). SEG2000a describe the assimilation of altimeter data only, using the Cooper and Haines scheme in the Hamburg Ocean Primitive Equation (HOPE) ocean model and demonstrate the improvement of ENSO forecasts at the European Centre of Medium-Range Weather Forecasts (ECMWF). The level of improvement relative to a control with no data assimilation was comparable to that achieved by assimilation of subsurface temperature observations only.

In this paper we describe a first attempt at ECMWF to combine the two data sources within the framework of OI. Carton et al. (1996), Carton et al. (2000), and Ji et al. (2000) have also used altimeter data in conjunction with other in situ observations such as from Tropical Atmosphere Ocean (TAO) array and expendable bathy thermograph (XBT) data. Our study differs from theirs in the strategy for using the altimeter data, and in that we assess the impact of altimeter data through an extensive set of ENSO forecasts based on the ocean analyses. In particular we update not only temperature (T), but also the salinity (S) field based on the local T-S relationship as described in Troccoli and Haines (1999) and Troccoli et al. (2001, hereafter TRO2001). Salinity variations in the equatorial west Pacific contribute to the sea level variations by as much as 9 cm (Ji et al. 2000; SEG2000a) and therefore a good representation of salinity is needed for the combined assimilation of temperature and sea level observations.

The paper is organized as follows. In section 2 we

describe the model and the assimilation schemes. In order to gauge the impact of different methods of assimilating data, a variety of assimilation procedures will be used. We will first describe assimilating altimetry in the absence of other data (section 2b). Assimilation of in situ temperature data will be described in section 2c. Combined in situ and altimeter assimilation is described in section 2d. A method to correct salinity based on the updated thermal field is described in section 2e. In section 3 we discuss the results from the various ocean analyses, and in section 4 the results from the coupled forecasts. Conclusions are given in section 5.

## 2. The assimilation system

### a. The ocean model

The oceanic component of the coupled ocean-atmosphere forecast system at ECMWF is a modified version of the HOPE model. The model has been developed at the Max Planck Institute for Meteorology and is described in detail by Wolff et al. (1997). The model uses an Arakawa E grid with a zonal resolution of  $2.8125^\circ$  at all latitudes. To allow a better representation of tropical waves, the meridional resolution is refined to  $1/2^\circ$  within  $10^\circ$  of the equator. Poleward of  $10^\circ$  the meridional grid spacing increases linearly to  $2.8125^\circ$  at  $30^\circ$  latitude and remains at that resolution poleward thereof. The uppermost 12 layers are centered at 10, 30, 51, 75, 100, 125, 150, 175, 206, 250, 313, and 425 m. The model time step is 2 h. Sea level is computed as a prognostic variable.

### b. The altimeter assimilation procedure

For the assimilation of altimeter data we use the method developed by Cooper and Haines (1996, henceforth CH96) to project the sea level observations onto the model's subsurface temperature and salinity fields. CH96 has the advantage that, as compared to statistically derived relationships between sea level displacement and subsurface temperature only (as used in Fischer et al. 1997; Carton et al. 1996; Ji et al. 1998, 2000; Masina et al. 2000), temperature and salinity increments are based on the model's T and S profiles at the time and location at which the observation is assimilated. Vertical shifts of the T-S profiles are used to update the model's temperature and salinity fields. The magnitude of the shifts is such that the depth-averaged change of weight of the water column after assimilation compensates for the difference between simulated and observed sea level. The CH96 scheme is able to capture advective changes in water-mass properties, which statistically derived projection schemes are not, as they are based on time-averaged variability at a fixed location. More recently efforts are being made to include seasonal variations in the correlation coefficients between temperature and sea level anomalies for the statistically derived projection (e.g., Masina et al. 2000).

CH96 is designed to correct displacements of the density structure that are caused by model errors or errors in the forcing fields such as wind. Potential drawbacks of the scheme are that it is not able to correct for steric sea level changes nor for errors in the freshwater input nor for errors in the model's water-mass characteristics. However, some of these changes may be better identified from other data sources such as in situ temperatures. The implementation of the assimilation procedure for altimeter data into the HOPE ocean model is described in detail in SEG2000a but a brief description is given here. Every 10 days, maps of SLAs relative to the 1993–95 period are produced by Centre Localisation Space, located in Toulouse, France. From early 1998, maps are available weekly. The latter maps are derived from the TOPEX/Poseidon and *ERS-1/2* satellites, and have a spatial resolution of  $0.25^\circ \times 0.25^\circ$  (LeTraon et al. 1995, 1998). At ECMWF the maps are smoothed because the ocean model has too coarse a resolution to resolve the eddies contained in the data. The maps are then interpolated to the model grid, where a mean sea level is added to the anomalies. The mapped data are assimilated every 10 days using CH96, and the derived temperature and salinity increments are spread over the following 10 days to allow a smooth adjustment of the density field.

The above method requires the initial interpretation of SLA in terms of  $T_{\text{sub}}$ . The CH96 method that we use requires a mean sea level, which is not yet provided with satellite observed sea level. We have taken this mean sea level, for the years 1993–95, from a former subsurface T assimilation experiment with the ocean model (denoted OI-3 in SEG2000a). Having to use a model-derived mean sea level in the assimilation process is a weakness in present attempts to assimilate altimeter data, preventing its full potential from being realized. This deficiency should be overcome once a sufficiently accurate geoid is available to provide absolute sea level observation from space. Such an accurate geoid should be available from gravimetric satellite missions within the next few years. The successful launch of the Catastrophes and Hazard Monitoring and Prediction (CHAMP) mission in July 2000 represents a useful start to this process that will continue with the Gravity Recovery and Climate Experiment (GRACE; launch 2002) and the Gravity and Ocean Circulation Experiment (GOCE; launch 2004) missions. In the meanwhile we accept the limitation of not having a measured mean sea level. This problem exists in all present attempts to use altimeter data, although it can be disguised if only temporal information is used.

### *c. Assimilation of subsurface temperature observations*

Subsurface temperature observations are presently assimilated into the ocean analysis via an optimum interpolation scheme (Smith et al. 1991). For the experiments

in this paper, manually quality controlled observations including XBT, conductivity–temperature–depth (CTD), and TAO data are used. Every 10 days, observations are collected over a centered 10-day period. The observed profiles are interpolated onto model levels. The optimal interpolation scheme is then solved independently for each model level. Individual observations and the modeled background are given the same weight. Differences in the weight of, for example, TAO relative to XBT are then determined by the number of observations in any time/space window. Because the TAO moorings provide daily data at the same location, relatively strong weight is given to TAO observations compared to XBT observations. The latter are mainly along ship tracks and therefore more than 2 or 3 XBT observations are seldom found within the background error decorrelation radius over a 10-day window.

The background and observation error spatial structures are modeled using Gaussian functions. The background error scales define the spatial extent of the area over which the correction from a single observation is applied. Background error decorrelation scales are anisotropic and vary with latitude. Based on the study of Meyers et al. (1991), at the equator the zonal scale is 1500 km and the meridional scale is 200 km. As latitude increases the zonal scale decreases and the meridional scale increases to 400 km in both directions at  $20^\circ$ . The observation error scale is defined as the typical spatial and temporal separation beyond which the errors of two individual observations become uncorrelated. More practically the observation error scale is used to filter out unwanted small-scale and high-frequency variability (like internal gravity waves) that are present in the observations. The observation error decorrelation scale is homogeneous and isotropic, with a space scale of 200 km and timescale of 3 days.

Once the analysis has been computed, the derived temperature increments are applied over the next 10 days to minimize adjustment problems. In this original temperature OI scheme, there is no correction to salinity. This can give rise to unreasonable temperature profiles as discussed by TRO2001. The main difference compared to the assimilation of sea level data is that assimilation of temperature observations is capable of correcting the vertical temperature structure, while sea level assimilation using CH96 can only correct misplacements of the temperature profile in the vertical. The major drawback is the sparseness of data, especially outside the domain of the TAO array. On the other hand, satellite observations span a near-global domain and have better spatial coverage even within the equatorial region, though their temporal resolution is worse than for TAO.

### *d. Combined assimilation of sea level and temperature observations*

In the following, we aim to combine the advantages of using altimetry and in situ temperature observations.

In so doing, we first assume that the directly observed temperature profiles are the more reliable source of information about the subsurface temperature field wherever such observations exist. The information from the altimeter is then mainly used in areas where few direct temperature observations exist, such as in the tropical Atlantic and Indian Oceans and outside the TAO array in the Pacific. The sea level observations are also used to update the salinity field over the whole model domain using the information about salinity provided by the CH96 scheme. Our approach thus differs from the approach of Vossepoel et al. (1999) who also have made attempts to combine the information from sea level and temperature data. Their approach is to use the history of sea level and salinity information to derive subsurface salinity at temperature profile observation points only. While their method may provide a better estimate of salinity for these limited locations, it requires not only in situ temperature observations but also a past history of salinity observations, which further limits the locations in which their analysis can be performed. Ji et al. (2000) have also combined temperature and sea level assimilation, but projected the entire sea level signal on the temperature field.

An optimum method to combine the altimeter and thermistor data has probably yet to be found. Based on a number of attempts regarding the order in which the observations are used, and whether to use smoothed or unsmoothed altimeter data, we chose the following approach for our global ocean analysis. We first analyze temperature and salinity from the altimeter data for every grid point using CH96 as described above. The altimeter-derived temperatures are not directly used to update the background field, however. Instead, the altimeter-derived temperatures are used as pseudo or synthetic temperature observations that are combined in the OI with the in situ temperatures from TAO/XBT and the model background. We thin the pseudotemperature observations before the OI. Every second latitude band is dropped in an initial step. In a second step, we check for each of the remaining grid points, whether an in situ temperature observation is present in the surrounding  $2^\circ \times 2^\circ$  box. If so, the respective pseudoobservation is dropped (a schematic is given in Fig. 1). Because the "exclusion box" is smaller than the decorrelation scales used for the OI, in particular close to the equator where the zonal decorrelation scale is 1500 km, there is still influence from the altimeter at in situ temperature observation points, but the weight given to the altimeter data is smaller because of the greater distance.

#### e. Correction of subsurface salinity

As outlined above and described in detail in TRO2001, the assimilation of only temperature data without correction of the model salinity field can introduce first-order errors in the temperature field. These errors can be substantially reduced when salinity is up-

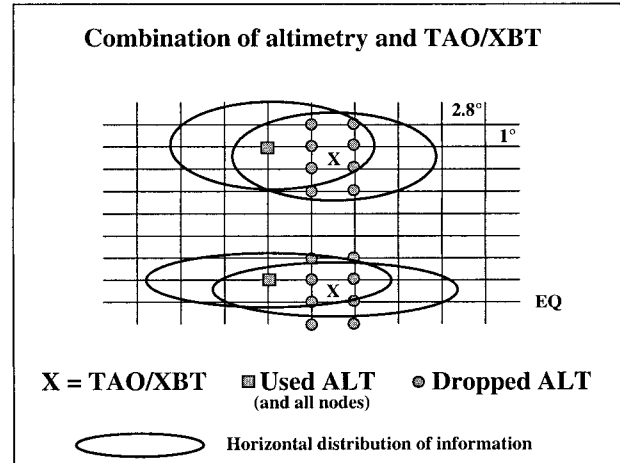


FIG. 1. Schematic of the horizontal filtering of the pseudo-observations.

dated together with temperature. Furthermore the importance of salinity was drawn to our attention by recent studies, which showed that subsurface salinity variations impact strongly on sea level variations in the western equatorial Pacific (e.g., Ji et al. 2000) and in the western equatorial Atlantic (Segsneider et al. 2000b). Because salinity observations are sparse, in particular those available in near-real time, it is not possible to analyze S based on direct measurements. However, an indirect approach that locally uses the T-S relationship of the background field to find the salinity that matches the newly analyzed temperature at each level has been developed by Troccoli and Haines (1999, hereafter TH99).

The improvements from using TH99 on the temperature fields when only temperature was assimilated have already been described in TRO2001. The ocean analysis was improved in particular in regions of pronounced salinity maxima at intermediate depth, such as in the western equatorial Pacific and Atlantic Oceans. However, most of the improvements of the temperature fields were achieved at depths of more than 200 m, and it is thus not immediately clear what the impact on seasonal forecasts might be. Here we apply TH99 in the presence of temperature and altimeter data and we will examine not only the ocean analyses, but also the impact on coupled forecasts. Adverse changes in T or S below the pycnocline may not directly affect the SST and propagation of upper-ocean heat content anomalies and hence the forecasts. They influence the sea level, however, and through that, prevent the optimum use of altimeter data. Hence we will show that application of the T-S scheme is considered necessary.

### 3. Ocean analyses

#### a. Setup of experiments

In the following, we will briefly describe the setup of the four ocean analyses that are used in the paper to

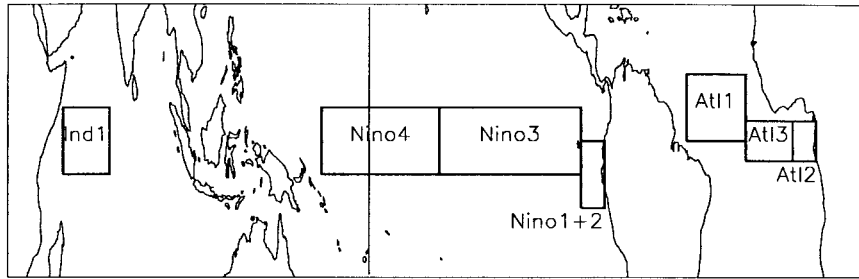


FIG. 2. Location of the various index areas that are used. The EQ1–EQ3 areas divide the area of Niño-3 and Niño-4 boxes into thirds. The latitudes and longitudes of the areas are given in the text.

gauge the impact of the different assimilation approaches. All four experiments are run for the five years 1993–97, that is, for the same period as the ocean analyses in SEG2000a. The initial conditions are taken from a former ocean analysis, in which TAO and XBT data were assimilated daily, and SST was relaxed strongly toward observed values (experiment OI-3 in SEG2000a). The ocean model is forced by daily averages of momentum, precipitation minus evaporation, and heat flux derived from the ECMWF reanalysis (now known as ERA-15) for 1993, and from the operational numerical weather prediction system for 1994–97. The model SST is relaxed to weekly averaged analyses of SST (Reynolds and Smith 1995) with a timescale of 3 days, and the sea surface salinity is relaxed to climatological data from Levitus and Boyer (1994) and Levitus et al. (1994) with a timescale of 1 month. Subsurface temperature and salinity are both relaxed to climatological data with a timescale of 1 yr. The OI is applied down to model level 15 (approximately 1000 m).

In the first experiment, called T-OI, only subsurface temperatures are assimilated (experiment OI-1 in SEG2000a). In a second experiment, called ALT, only altimeter data are assimilated (experiment ALT-5 in SEG2000a). In the third experiment, called T + A, both altimeter and temperature observations are assimilated as described in section 2d. In experiments ALT and T + A, the salinity increment from the sea level assimilation is used to update salinity at all model grid points. In the fourth experiment, called TA + TS, temperature and sea level are assimilated as in T + A, but salinity is corrected using the TH99 scheme described in section 3e.

Experiments T-OI and ALT have already been described in SEG2000a and are mainly used as a reference in this paper. In particular, we will use Niño-3 and Niño-4 averages of the depth of the 20°C isotherm (D-20) in experiment T-OI as references for the observed subsurface temperature. These are directly assimilated in T-OI and the TAO network provides relatively good coverage with observations. It is not trivial to define the observed true state of D-20 averaged over Niño-3 or Niño-4, however. Deviations between T-OI and T + A (i.e., altimeter data added) could also be caused by spatial variations of D-20, which are observed by the al-

timeter that has high-spatial sampling density, but are missed out by the TAO array. On the other hand, TAO provides better temporal density. XBTs offer the best vertical resolution, but have poor spatial and temporal density. An ocean analysis of the equatorial Pacific is performed routinely at the Bureau of Meteorology Research Centre and could be used for verification, but it uses basically the same OI scheme as T-OI to fill the gaps between the observations and may also deviate from the true state. Experiment ALT is used as a reference for sea level. From earlier comparisons it was shown that the sea level of experiment ALT is close to the observed sea level in the Tropics (SEG2000a).

#### b. Results from the ocean analyses

In this section, results from the ocean analyses will be described. Our main emphasis is on upper-ocean heat content as represented by D-20 and the sea level, which will be shown relative to the global mean. We shall show results for the tropical Pacific, Atlantic, and Indian Oceans for the index areas shown in Fig. 2. In the following time series the sea level from experiment ALT and D-20 of experiment T-OI, respectively, will be drawn as solid black lines, as they will be taken as references.

We will start with the tropical Pacific. In the Niño-3 region (5°S–5°N, 90°–150°W, Fig. 3) the sea levels (Fig. 3a) in all experiments agree to within 2–3 cm. The deviations of D-20 between experiments are generally smaller than 5 m, though on occasion they can reach 10 m, as in experiment ALT in 1995 for example (Fig. 3b). The generally good agreement between the different experiments indicates first that the assimilation of sea level is able to constrain the thermocline well, and second that the assimilation of subsurface temperature constrains the sea level well. By combining the two observation types, the departures of D-20 of experiment ALT from the reference can be further reduced in experiments T + A and TA + TS as seen in Fig. 3b. The most pronounced feature in Fig. 3 is the strong rise in sea level and the deepening of the thermocline in 1997. Comparing Figs. 3a and 3b, one can see that while the deepening of the thermocline is associated with a gen-

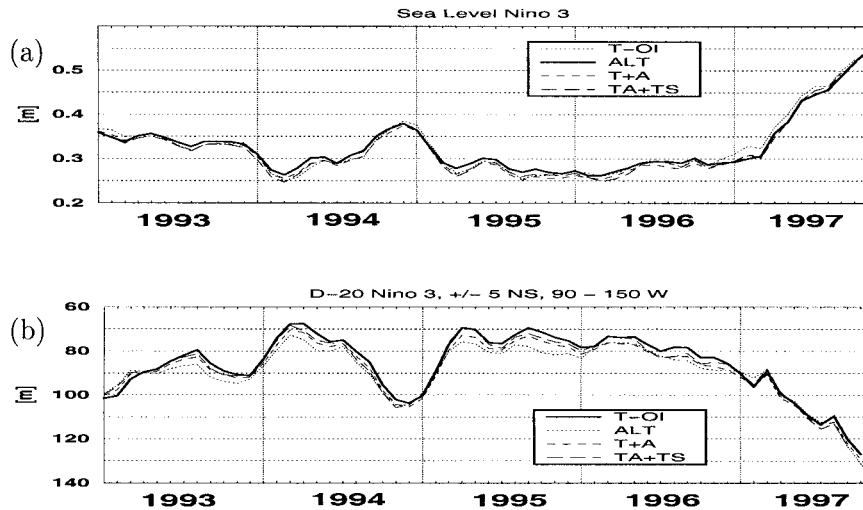


FIG. 3. Time series of (a) sea level and (b) D-20 averaged over the Niño-3 region from experiments T-OI, ALT, T + A, and TA + TS.

eral rise of sea level the two figures are not precisely mirror images of each other. This implies that it is not always adequate to use sea level as a proxy for thermocline depth as is sometimes done in altimeter assimilation. The good representation of D-20 in experiment ALT, where only altimeter data are assimilated, underlines the ability of the model to reproduce the time-varying temperature structure and the strength of the CH96 scheme that actually takes the vertical structure of the model temperature field into account.

In the Niño-4 region ( $5^{\circ}\text{S}$ – $5^{\circ}\text{N}$ ,  $150^{\circ}\text{W}$ – $170^{\circ}\text{E}$ , Fig. 4) the agreement for the D-20 time series is again excellent, and what little deviation there is in the altimeter-only assimilation experiment (ALT), is further reduced by the additional assimilation of temperature observations in experiments T + A and TA + TS, as one would

expect. For the sea level in Niño-4 where salinity variations contribute more to sea level changes than in Niño-3, the agreement between the experiments is slightly worse than for the Niño-3 region. Beginning during the second half of 1995 and through until mid-1997 the sea level is too high in experiment T-OI compared with the reference experiment ALT, with differences in the range of 5 cm. This period has been discussed at some length by Ji et al. (2000) who noted the importance of salinity. One would expect that the additional correction of salinity in experiment TA + TS should improve the sea level, but in fact the sea level is more similar to that of T-OI than to ALT over the relevant period, whereas experiment T + A agrees quite well with experiment ALT. Kessler (1999) argues that salinity in the western Pacific changed due to the hor-

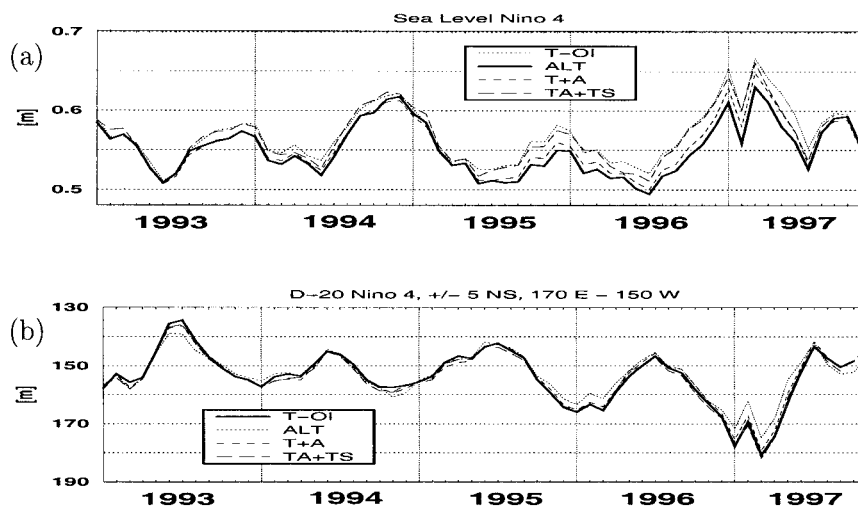


FIG. 4. Time series of (a) sea level and (b) D-20 averaged over the Niño-4 region from experiments T-OI, ALT, T + A, and TA + TS.

zontal advection of saltier water from the east. The TH99 scheme searches for the matching salinity in the vertical and cannot correct the salinity error of the model, and as a consequence the sea level is similar to that of experiment T-OI. An improved version of TH99 that also searches in the horizontal is under development, but has not yet been tested in a tropical application.

In the Atlantic, standard regions are less commonly used than in the Pacific, but we adopted the three regions defined by Zebiak (1993). These are: ATL1 from the equator to 10°N, and from 20° to 45°W, ATL2 between plus and minus 3°N/S and 0–10°E, and ATL3, which spans the region between plus and minus 3°N/S and 0°–20°W. In the Atlantic, it is less likely than in the tropical Pacific that the temperature and D-20 from experiment T-OI can serve as a robust measure of truth, since in situ temperatures are less frequently observed and hence constrain the analysis less well. It has even been shown that the OI analysis using temperature only had severe errors in the western tropical Atlantic, which showed up after the introduction of the PIRATA moorings (Segschneider et al. 2000b). We therefore use results from a former control experiment in which no data have been assimilated (experiment CNT in SEG2000a). We do not show the time series of CNT in the figures to keep them more readable, but will describe results instead. Experiment CNT is used to evaluate the impact of the temperature assimilation on sea level in the Atlantic and Indian Oceans. If the sea level from the assimilation experiment T-OI shows larger departures from the reference experiment ALT than the control run, we can suspect the temperature fields of T-OI are in error, although the evidence is not fully conclusive.

The sea level in the western equatorial Atlantic (ATL1 region, Fig. 5a) shows considerably less interannual variations than in the Pacific. The time series are dominated by the seasonal cycle and agree within 1 cm between experiments ALT, T + A, and TA + TS. The seasonal cycle of the temperature-only assimilation experiment T-OI is slightly phase shifted with respect to experiment ALT, that is, the sea level in T-OI is highest in November–December rather than in September–October as in ALT. The same feature is present in the control, which suggests an error in the forcing fields or model formulation, the effects of which on the ocean analysis are not corrected by the sparse temperature observations in the Atlantic in T-OI. The sea level of experiments T-OI and the control run differ by up to 3 cm from the altimeter-derived sea level. The sparsity of thermal data means that the depth of the 20° isotherm of experiment T-OI might also be in error (Fig. 5b). The sea level of T-OI and the control experiment are quite similar, but D-20 is almost 10 m deeper in the control experiment than in T-OI. The analyses incorporating altimeter data differ from experiment T-OI by only a few meters for most of the time, but for example in spring 1995 D-20 in experiment T + A is almost 5 m shallower.

In the eastern equatorial Atlantic (ATL2 region, Fig.

5c) interannual variations in sea level are slightly more prominent than in the west (ATL1), but the dominant signal is the semiannual cycle with peaks in sea level around March and October. Again, the sea level of experiments ALT, T + A, and TA + TS agree quite closely, whereas experiment T-OI and the control run show deviations of more than 5 cm from the altimeter-derived sea level. The strongest deviations occur in spring, in particular during spring 1996. The phase of the sea level in the ATL2 region agrees well between all experiments. As for ATL1, experiment T-OI has the shallowest D-20, and the control experiment the deepest, with the experiments involving the assimilation of altimeter data having D-20 at intermediate depths.

In the central equatorial Atlantic (ATL3 region, Fig. 5e) both the seasonal cycle and interannual variability are weak. The minimum of sea level in the middle of each year is strongest in 1994 and weakest in 1996, but the difference is only 5 cm. The sea level from the experiments that assimilate altimeter data agree closely, whereas experiment T-OI deviates by more than 5 cm in particular in the spring of most years. The T-OI run shows the same behavior as the control, thus indicating that the seasonal cycle can not be corrected in T-OI, presumably due to the lack of temperature data. The variations in D-20 show larger differences than in the other regions. The three altimeter experiments are reasonably consistent but differ by up to 20 m from D-20 in the T-OI experiment. The pattern of variability in D-20 in T-OI is less well correlated with that in the altimeter experiments than is the case in the ATL1 and ATL2 regions. Since we know that assimilation of in situ temperature only can damage the thermal structure in this region (TRO2001; Segschneider et al. 2000b), there is scope for the altimeter-based analyses to provide a better estimate of the oceanic state.

In the equatorial Indian Ocean we introduce an index region, IND-1 defined as the area between 10°N/S and 50°–70°E. Figure 6a for this region shows that interannual variations of sea level are slightly larger than in the Atlantic. The variations are on the order of 10 cm for the sea level minimum in December, with lower than average values in 1996 and higher than average sea level in 1994. The agreement between the experiments is within a few centimeters with T-OI slightly too high. Variations of D-20 (Fig. 6b) are more dominated by a strong semiannual cycle. The differences between experiments can be 10 m. To put that into context the interannual variations are on the order of 15 m (between Nov 1994 and Nov 1996).

### c. Salinity

The role of salinity in the framework of temperature assimilation at ECMWF is discussed in detail by TRO2001. A brief discussion on the role of salinity when altimeter data are assimilated is given in SEG2000a and Segschneider et al. (2000b). Here we

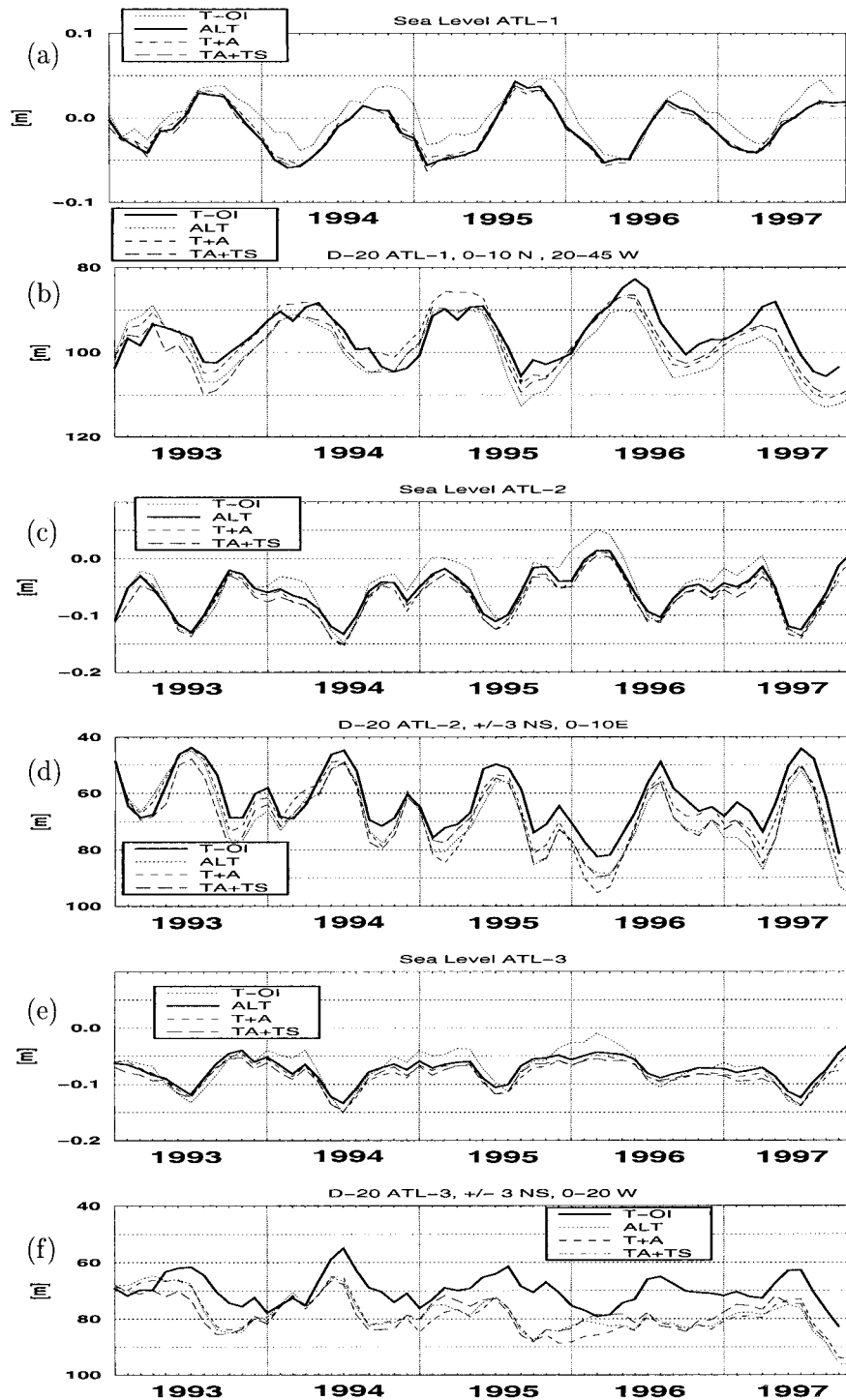


FIG. 5. Time series of (a) sea level and (b) D-20 averaged over the ATL-1 region, (c) and (d) for the ATL-2 region, and (e) and (f) for the ATL-3 region from experiments T-OI, ALT, T + A, and TA + TS.

will briefly discuss salinity for the experiments in which both sea level and subsurface temperatures are assimilated. We show average salinity integrated over the upper 300 m (S300), where most of the salinity variations

occur, for the Niño-3 and Niño-4 regions in Fig. 7. Differences in the integrated salinity result in differences of sea level and therefore impact on the altimeter data assimilation. The treatment of salinity during the assim-

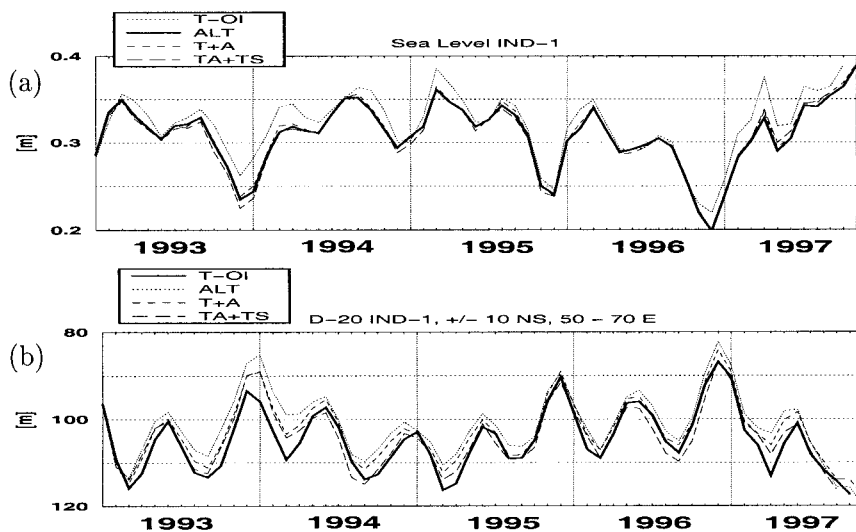


FIG. 6. Time series of (a) sea level and (b) D-20 averaged over the IND-1 region from experiments T-OI, ALT, T + A, and TA + TS.

ilation is as follows: in T-OI salinity is not updated at all, in experiment ALT and T + A salinity is updated using vertical shifts of the model background profiles based on sea level only, and in experiment TA + TS the TH99 scheme is used to correct salinity based on the analyzed temperature. When temperature observations are assimilated together with sea level, the vertical structure of the temperature fields can be altered, and the salinity fields of experiment T + A (using salinity from CH96) and TA + TS (using salinity from TH99) can be different.

Differences in S300 between the experiments are present but it is not straightforward to decide which of the four experiments performs best, as there is little salinity data for verification. In the Niño-3 region (Fig. 7a) the integrated salinity of experiment T-OI is lowest, and quite similar in experiments ALT, T + A, and TA + TS. From 1995 onward, experiments T + A and TA + TS are still quite similar, whereas experiment ALT has slightly higher salinity. In the Niño-4 region (Fig. 7b), T-OI shows less variability than the three other experiments. The differences between the averaged salinity for all experiments are less than 0.1 psu (practical salinity units) for both areas. This seems small but assuming an average temperature of 19°C and salinity of 35 psu, this translates into a sea level difference of slightly more than 2 cm (based on Table A3.1 in Gill 1979).

#### 4. Coupled forecasts

The following section will mainly follow the outline given in SEG2000a. Our principal aim is to provide optimum initial conditions for coupled ENSO forecasts. By comparing four sets of forecasts started from the experiments T-OI, ALT, T + A, and TA + TS, the

impact of the different assimilation methods on predicted SST anomaly (SSTA) is investigated. Two new sets of coupled forecasts were performed in addition to those discussed in SEG2000a, each set consisting of 100 forecasts over 6 months. In all cases the same version of the ECMWF atmospheric model was used (Cy15r8). One set of forecasts was initialized from the ocean analysis in which temperature and altimeter data were assimilated (coupled experiment named C-T + A), and a second set from the ocean analysis in which the T-S correction scheme was additionally applied (coupled experiment named C-TA + TS). Forecasts initialized from the assimilation of subsurface temperatures only (C-OI) and the assimilation of altimeter data only (C-ALT) are used as a reference. These two experiments are the same as discussed in SEG2000a. The improvements of C-OI and C-ALT with respect to the control forecasts that were started from an ocean analysis without subsurface data assimilation have already been demonstrated (SEG2000a) and therefore the control forecasts are not shown here. In the following, we will investigate whether the combined assimilation of subsurface temperatures and sea level, and the additional correction of the salinity field using the TH99 scheme, can further improve the forecasts.

For each experiment, 5-member ensembles were started on the first of January, April, July, and October of the years 1993–97. The ensembles were created by perturbing the SST of the initializing ocean analyses over predefined areas in the tropical Pacific. Although a fully dynamical coupled model is used to perform the forecasts, only the predicted SSTA in the Pacific will be discussed. This is mainly because we expect the largest impact from the data assimilation on the forecasts in this area, where the signal-to-noise ratio of interannual SST variations is relatively high. We will not address

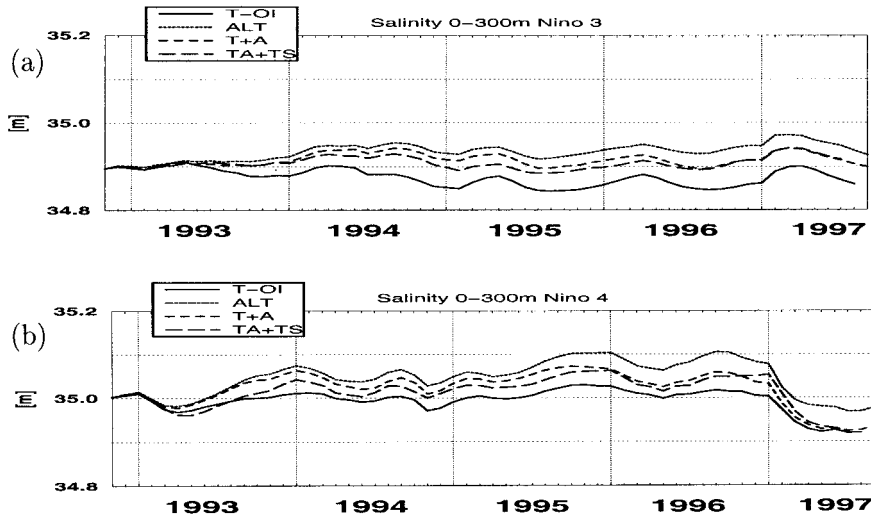


FIG. 7. Time series of salinity averaged over the upper 300 m for (a) the Niño-3 region and (b) the Niño-4 region from experiments T-OI, ALT, T + A, and TA + TS.

the prediction of atmospheric parameters such as precipitation that would require larger ensemble sizes.

Because we use a fully coupled model without flux correction, our model SST drifts. A linear estimate of this drift is computed a posteriori and subtracted from the predicted SST as discussed in Stockdale (1997). The drift is computed separately for the forecasts that are started in January, April, July, and October. Here we will discuss the differences of the drift between the various coupled experiments for the EQ-2 region (Fig. 8).

The drift is smallest for experiment C-ALT for all start months, and largest for experiment C-OI. The difference in the drift between C-OI and C-ALT after 6 months varies from 0.5°C for July starts up to 0.9°C for October starts. The initialization from the combined temperature and sea level ocean experiments results in intermediate drifts for experiment C-T + A and C-TA + TS. The impact of the TH99 scheme on the model drift is negligible, as the drift is very similar in experiments C-T + A and C-TA + TS. It is not a priori clear why

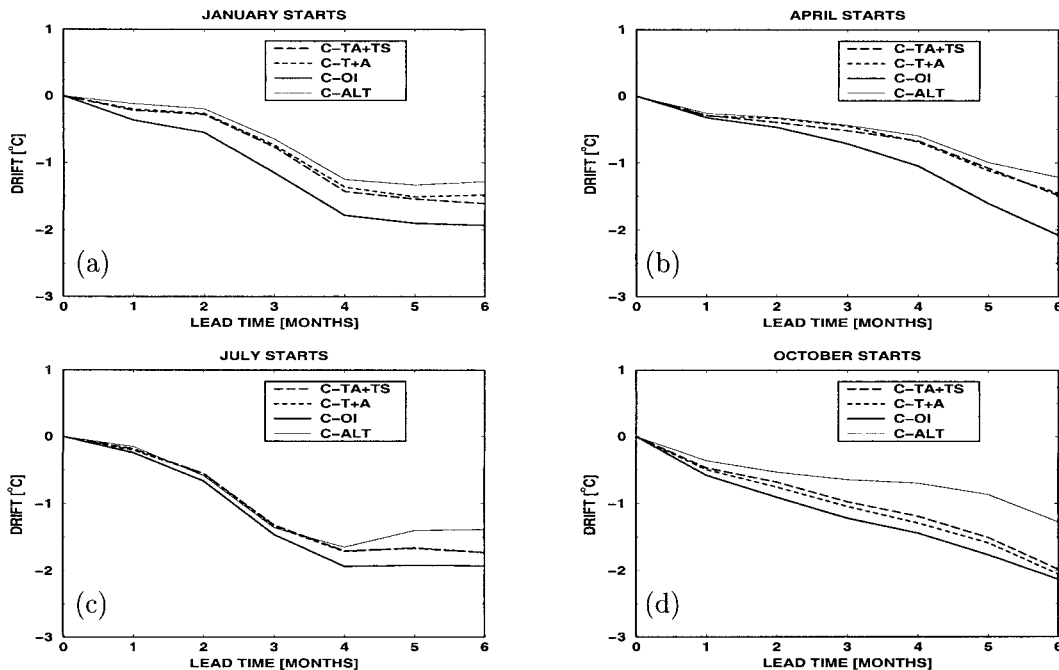


FIG. 8. Ensemble average of the coupled model SST drift averaged over the EQ-2 region (5°S–5°N, 130°–170°W) for experiments C-OI, C-ALT, C-T + A, C-TA + TS for forecasts started in (a) Jan, (b) Apr, (c) Jul, and (d) Oct.

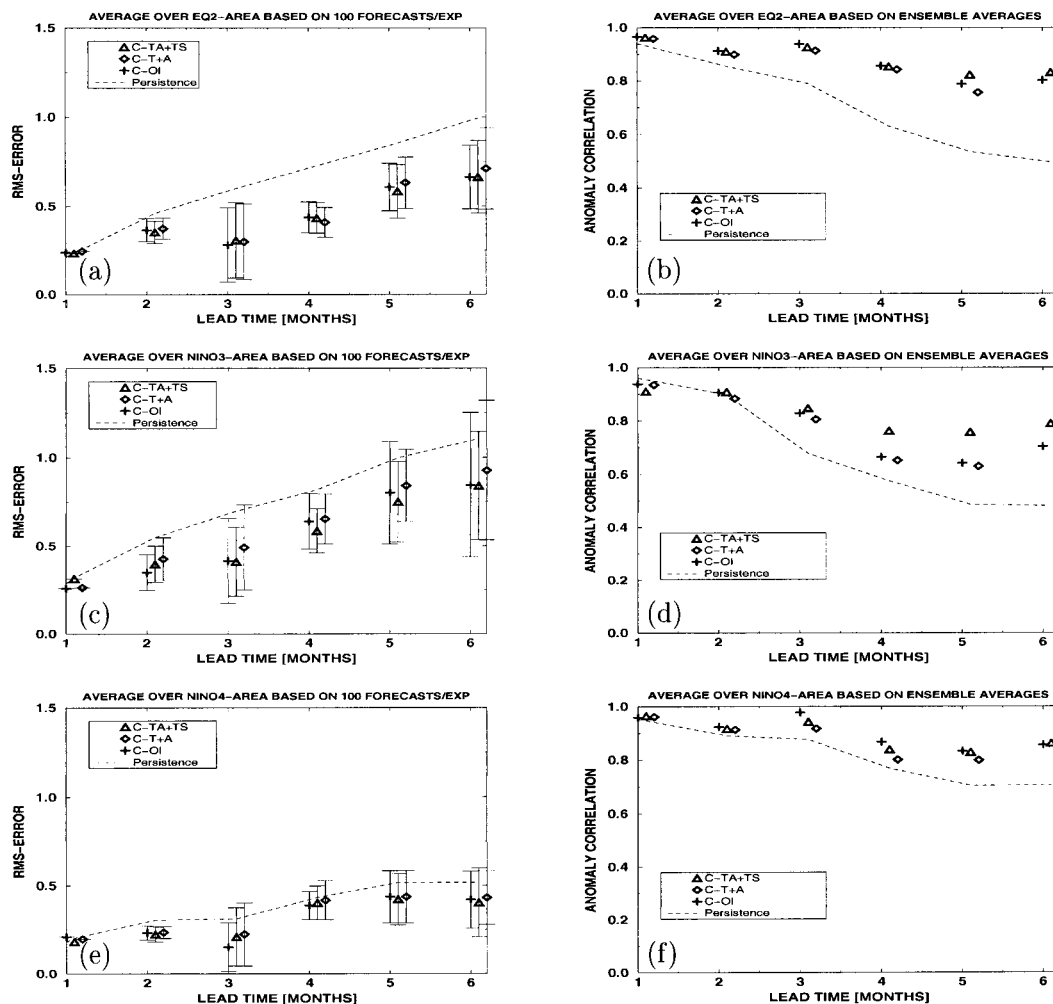


FIG. 9. Ensemble average of the SST rmse (left column) and the anomaly correlation coefficients of the ensemble mean (right column) averaged over (a),(b) the EQ-2 region ( $5^{\circ}\text{S}$ – $5^{\circ}\text{N}$ ,  $130^{\circ}$ – $170^{\circ}\text{W}$ ), (c),(d) the Niño-3 region ( $5^{\circ}\text{S}$ – $5^{\circ}\text{N}$ ,  $90^{\circ}$ – $150^{\circ}\text{W}$ ) and (e),(f) the Niño-4 region ( $5^{\circ}\text{S}$ – $5^{\circ}\text{N}$ ,  $150^{\circ}\text{W}$ – $170^{\circ}\text{E}$ ) for experiments C-OI (plus signs), C-T + A (diamonds), and C-TA + TS (triangles). The thin dashed line shows the persistence forecast. The symbols are offset to allow better readability.

the assimilation of the altimeter data alone in experiment C-ALT results in the smallest drift. Although it is desirable to have as little drift as possible, it is not a priori evident that a smaller drift in C-ALT results in better SST forecasts than for the other experiments as will be shown below. The impact of the reduced drift on the predicted precipitation can only be investigated with bigger ensembles than computed for this study.

The traditional measures of SSTA forecast skill, rms error (rmse) and anomaly correlation coefficient (ACC), are shown in Fig. 9 for experiments C-OI, C-T + A, and C-TA + TS as average over the EQ-2 (Figs. 9a,b), Niño-3 (Figs. 9c,d), and Niño-4 (Figs. 9e,f) regions. In SEG2000a, it was found that experiment C-OI (plus signs) performed best in terms of rmse and ACC compared to the control forecasts and the altimeter initialized forecasts. Any improvement of the skill from the combined assimilation of temperature and sea level in

C-T + A, and the additional application of the TH99 scheme in C-TA + TS, should therefore be measured against C-OI.

For the rmse in the EQ-2 region (Fig. 9a) such an improvement is not evident: all coupled experiments give very similar results. The deviations between them are less than  $0.05^{\circ}\text{C}$  even for a lead time of 6 months and are much smaller than the individual standard deviations that are on the order of  $0.25^{\circ}\text{C}$  (shown by the vertical bars). The ACCs of all coupled experiments (Fig. 9b) are on the order of 0.8 for 6 months lead, and are clearly better than for the persistence forecast (thin dashed line). The ACCs are very similar for all experiments. In the Niño-3 region the differences between the experiments are slightly larger for both rmse ( $0.1^{\circ}\text{C}$ , Fig. 9c) and ACC (Fig. 9d). Experiment C-TA + TS gives higher correlations than C-OI and C-T + A by almost 0.1 for lead times of 4–6 months. The rmse is

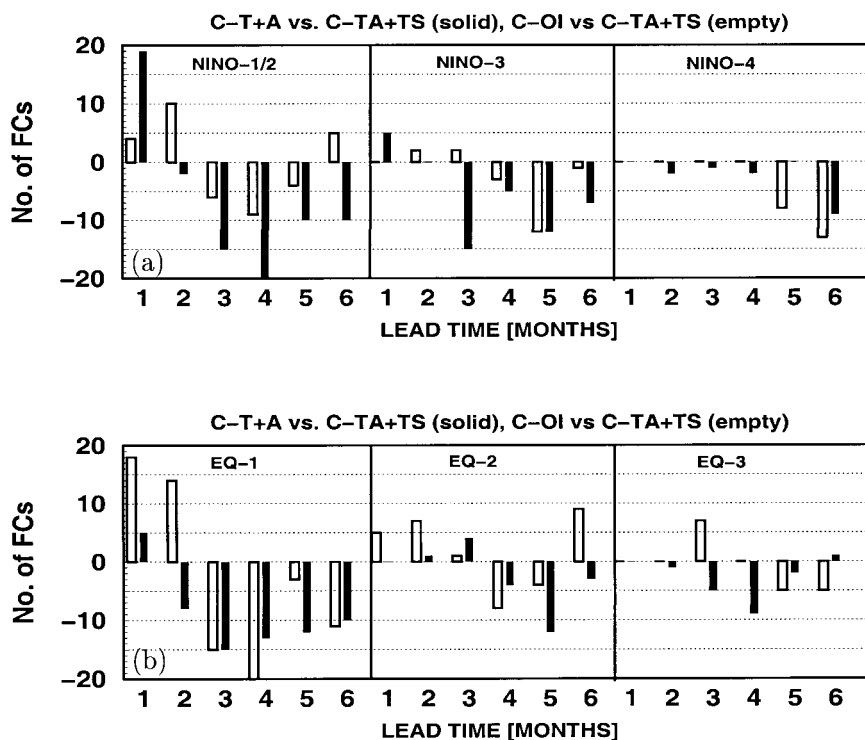


FIG. 10. Relative performance of the coupled experiments for the areas (a) Niño-1/2 ( $80^{\circ}$ – $90^{\circ}$ W), Niño-3 ( $90^{\circ}$ – $150^{\circ}$ W), Niño-4 ( $150^{\circ}$ W– $160^{\circ}$ E), and (b) EQ-1 ( $90^{\circ}$ – $130^{\circ}$ W), EQ-2 ( $130^{\circ}$ – $170^{\circ}$ W), and EQ-3 ( $170^{\circ}$ W– $150^{\circ}$ E). In all regions the latitudinal extent is  $5^{\circ}$ S– $5^{\circ}$ N except in Niño-1/2 where it is  $10^{\circ}$ S to the equator. A forecast (FC) is considered better if it is more than  $0.3^{\circ}$ C closer to the observed SSTA. Solid bars compare experiment C-T + A to C-TA + TS, and empty bars C-OI to C-TA + TS. Shown is the number of better minus the number of worse forecasts. Bars in the negative range mean that C-TA + TS performed on average better, bars in the positive range mean that it performed worse.

also smallest in C-TA + TS, but improvements are less clear than for the ACC. In the Niño-4 region where SST variations are smaller than in the eastern equatorial Pacific, deviations between the experiments are again small for both rmse (Fig. 9e) and ACC (Fig. 9f). According to a Wilcoxon–Mann–Whitney test, however, none of the differences is significant at a level of confidence of more than 70%.

The next skill measure is what we define as the relative performance of pairs of forecast sets. A set of forecasts is “better” if it is closer to the observed SSTA by more than a specified threshold value, which here is chosen to be  $0.3^{\circ}$ C. The basic motivation to define this skill measure is that for some applications of El Niño forecasts, it might be more important to know which forecast system is closest to the observations on most occasions rather than how the rmse for the whole set of forecasts performs. For instance so-called weather derivatives are based on the number of days when the temperature exceeds or falls below a certain value, in which case an insurance company will pay an amount of money that can be used for instance by a brewery to reduce losses in a colder than average summer when the beer gardens are empty. For such a product it is of

no importance how wrong or right a forecast is, but only whether the temperature is correctly predicted above or below that threshold.

Such a measure is given in Fig. 10 for six regions in the equatorial Pacific. It is of interest that, while the Niño regions and the EQ regions cover almost the same equatorial belt, longitudinal shifts of the boxes can sometimes result in significantly different skill estimates. First, experiments C-OI and C-TA + TS are compared (empty bars), that is the impact from the additional assimilation of sea level observations and the correction of salinity compared to the assimilation of temperature data only. On average C-TA + TS performs better than C-OI for lead times of more than 3 months, with exceptions for a lead time of 6 months in EQ-2 and Niño-1/2. On shorter lead times, C-OI performs relatively better compared to the longer lead times (e.g., C-OI is better than C-TA + TS in the EQ-1, EQ-2, and EQ-3 regions for up to 2 months ahead). Second, experiments C-T + A and C-TA + TS are compared (solid bars), that is the impact of the TH99 correction of salinity is estimated. Figures 10a,b show that for almost all areas and lead times, C-TA + TS performs better than C-T + A. This implies that a good simulation of

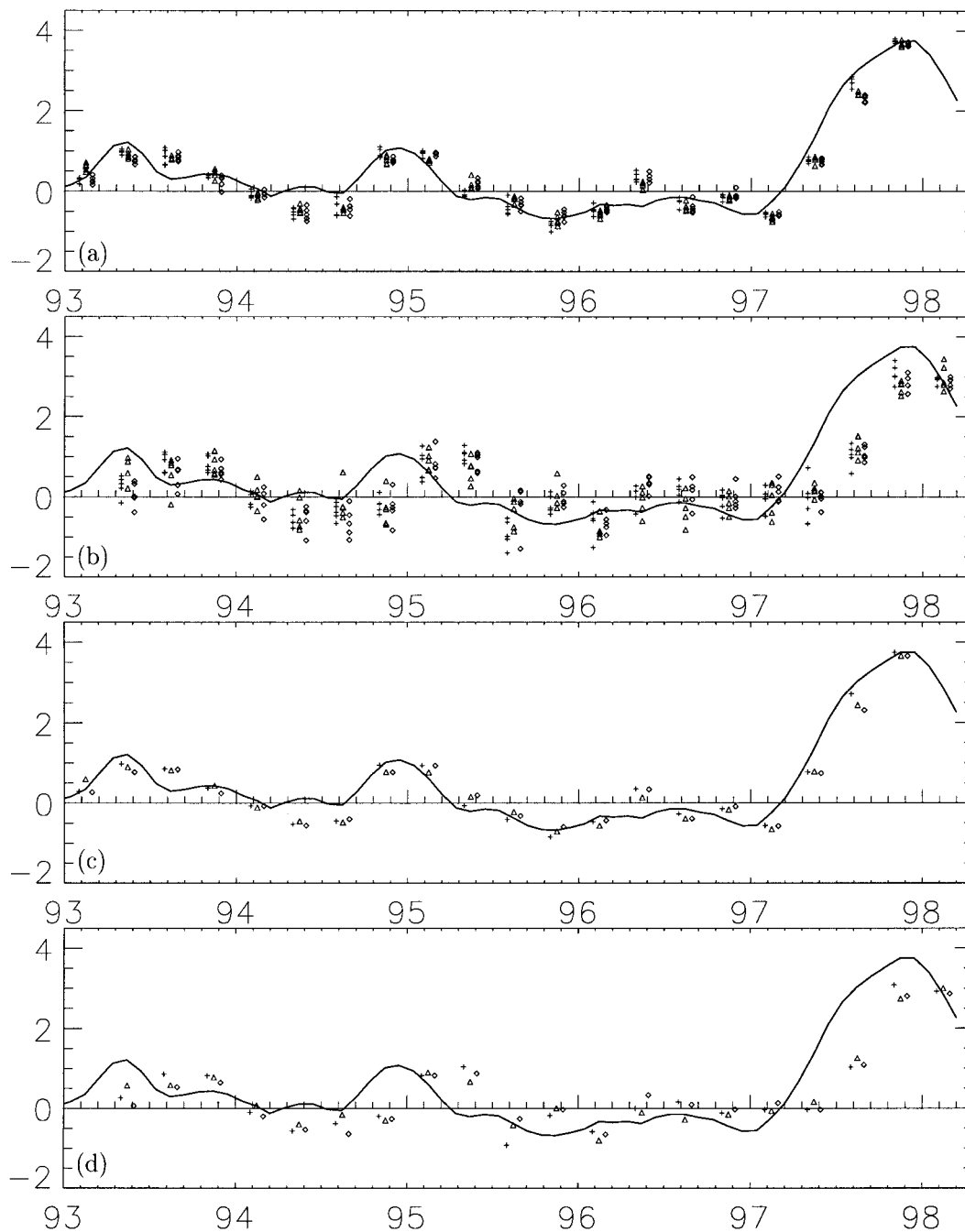


FIG. 11. The 3-month means of predicted SST anomalies ( $^{\circ}\text{C}$ ) averaged over Niño-3 and observed SST anomaly for (a) ensemble members 1–3-months lead, (b) ensemble members 4–6-months lead, (c) ensemble mean 1–3-months lead, and (d) ensemble mean 4–6-months lead. The + indicates experiment C-OI (offset  $-14$  days),  $\Delta$  experiment C-TA + TS, and  $\diamond$  experiment C-T + A (offset  $+14$  days). The solid line is the observed SST anomaly.

the salinity field is required to make optimum use of the altimeter data.

In the next approach, we compare 3-month means of predicted and observed SST anomalies averaged over the Niño-3 region (Fig. 11) and Niño-4 (Fig. 12). The 3-month means represent seasonal averages. Shown are experiments C-OI (plus signs), C-T + A (diamonds),

and C-TA + TS (triangles). Figures 11a,b and 12a,b show the individual ensemble members, for (a) 1–3-months lead time and (b) 4–6-months lead time. Figures 11c,d and 12c,d show the ensemble averages for (c) 1–3-months and (d) 4–6-months lead time. The thin line is the 3-month running mean of the observed SST anomaly relative to the 1950–79 climatology.

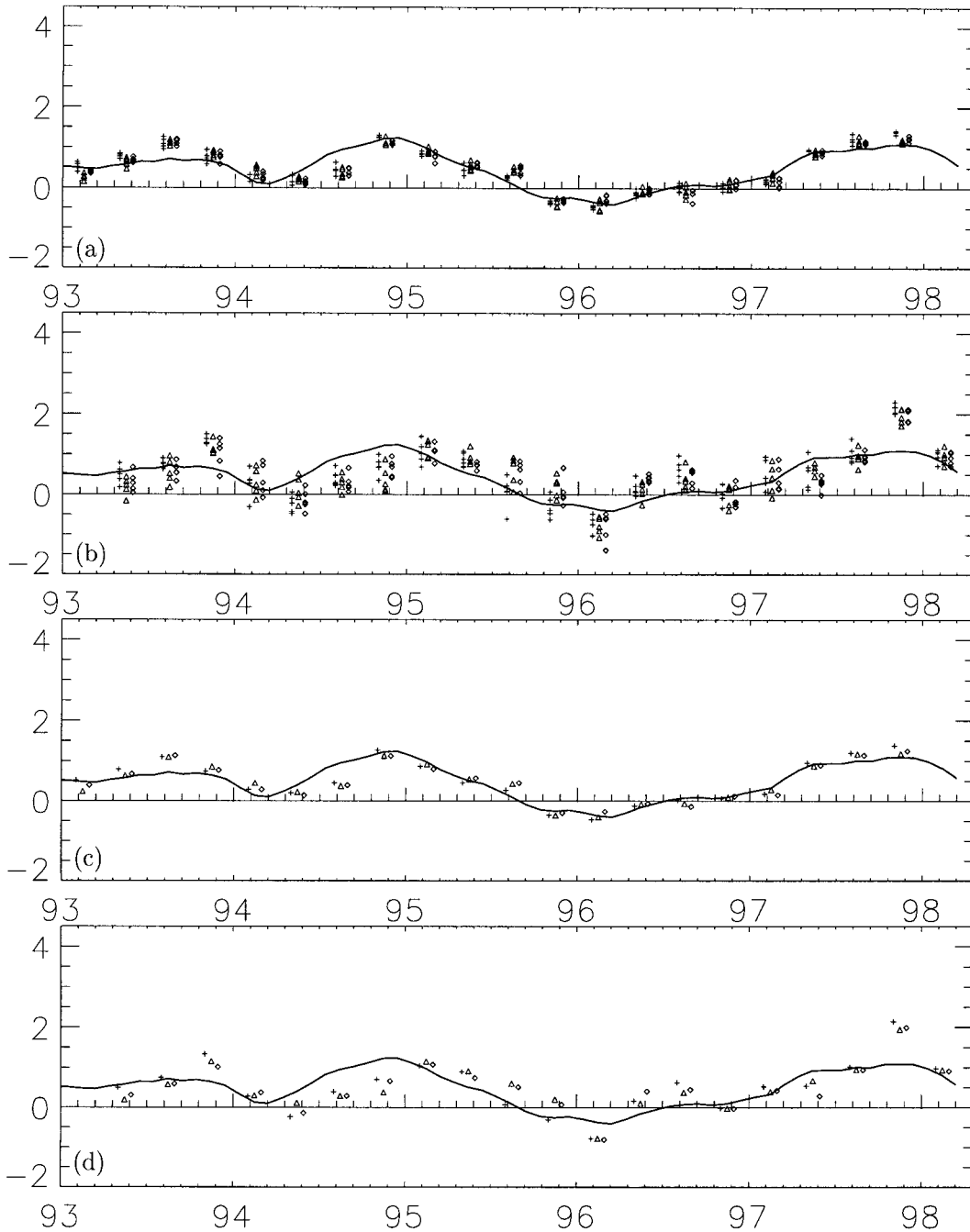


FIG. 12. as Fig. 11, but for the Niño-4 region.

Given that we use a probabilistic forecast system, one method to declare a forecast right or wrong is to check whether the ensemble of predicted values includes the observed SSTA. We will start with the Niño-3 region and 1–3-month lead time (Fig. 11a). Even though in general, the fit between predicted and observed SSTA is fairly close, for most of the time none of the forecast experiments satisfies this objective. One possibility is that the ensemble spread of the forecasts, which is gen-

erally less than  $0.3^{\circ}\text{C}$ , is too small for short lead times. We hope that this will be improved in the next generation forecast system by using new mechanisms to generate the ensemble.

For 4–6-month lead time (Fig. 11b) the ensemble spread for Niño-3 SSTA forecasts is generally on the order of  $1^{\circ}\text{C}$  and thus considerably larger than for 1–3-month lead, but so is the forecast error. It is therefore not a priori clear whether the range of the predicted SST

includes the observed SST more often for longer lead times. We counted the number of forecasts for which the range of the ensemble of predicted SSTA includes the observed SSTA based on Figs. 11a,b. For 1–3-months lead the observed SSTA is covered for 9 forecast dates in experiment C-OI, for 7 dates in C-T + A, and in only 4 cases for C-TA + TS. For 4–6-month lead the distribution is 8:9:12 (C-OI:C-T + A:C-TA + TS). The conclusion from this comparison is that for Niño-3 SSTA forecasts, C-OI performs best for shorter leads and C-TA + TS for longer leads, which is consistent with the previous test.

Ensemble averages of predicted SSTA for Niño-3 are shown in Figs. 11c,d and for Niño-4 in Figs. 12c,d. The ensemble averages of SSTA in the Niño-3 and Niño-4 regions are used to derive rates of false alarms and hit or missed events. The false alarms, and hit and missed events are defined as in SEG2000a: first, an event is defined as a 3-month average SSTA of more than  $\pm 1^\circ\text{C}$ . A false alarm is defined as a predicted event when no event is observed, and when the forecast error of SSTA is larger than  $1^\circ\text{C}$ . An event is declared “missed,” if an observed event is underpredicted by more than  $1^\circ$ , and declared “hit” if it is predicted within  $\pm 0.2^\circ\text{C}$ .

The following numbers are total numbers for Niño-3 and Niño-4, and 1–3- and 4–6-month lead. The hit rates distribute as 10:9:9 (again for C-OI:C-T + A:C-TA + TS), the false alarm rate as 2:1:0, and the missed events as 3:5:5. The number of false alarms is reduced in experiment C-TA + TS. The improvements for the two forecasts when false alarms occur (for Niño-3 and Jun 1995 and Niño-4 for Nov 1997, both 4–6-month lead) are only small, however.

## 5. Conclusions

In this paper we have described our first attempts to combine assimilation of altimeter and temperature profile observations in the framework of seasonal forecasting. Four sets of ocean analyses and coupled forecast experiments have been considered. Two of these were already discussed in SEG2000a; namely, the assimilation of in situ thermal data only and the assimilation of altimeter data only. Our aim here is to assess the added value from combining altimeter data with our existing in situ temperature data assimilation system. Two new ocean analyses using the combined observations were performed that differed only in the way that salinity was estimated. In one experiment salinity is corrected based on each new temperature analysis and a preservation of the local T–S relationship, in the other based directly on the altimeter data, using vertical shifts of the background profile. These two different combined analyses can be thought of as the addition of altimeter data to two different in situ analysis systems, one of which adjusts salinity based on the temperature analysis and the local T–S relationship, and one of which makes no adjustment. The desirability of correcting salinity when

updating temperature has nothing to do with altimeter data per se. Errors in the salinity field, however, can have an impact on the model sea level, and through that prevent an optimum use of the altimeter data.

In the Pacific, the differences between the four ocean analyses are usually quite small as measured by D20 and sea level. For both Niño-3 and Niño-4, the differences in D20 are generally less than 10 m, which is considerably less than the scale of interannual variability that can be 70 m in Niño-3 and 50 m in Niño-4. The differences between OI with and without altimetry are generally less than 5 m. The sea level differences in Niño-4 are proportionately larger than the D-20 differences: 5 cm between experiments compared to interannual changes of 15 cm. These differences may reflect changes arising from the different ways salinity is handled in the various experiments.

In the equatorial Atlantic Ocean, the differences of upper-ocean heat content between the four ocean analyses are larger than in the equatorial Pacific. In the equatorial Indian Ocean, differences are of intermediate magnitude. Even if the altimeter provides good data coverage in the Indian and Atlantic Oceans, the success of the assimilation of sea level observations relies on the subsurface temperature structure of the model that is used to project the sea level information onto the temperature field. In the equatorial Atlantic and Indian it is more difficult than in the Pacific to obtain even a sparsely observed state of the subsurface temperature field. This should improve in the near future: observations from the Pilot Research Moored Array in the Tropical Atlantic (PIRATA) already provide information of the subsurface temperatures in the tropical Atlantic, and observations from ARGO floats (a global array of profiling floats) should become available in near-real time soon.

We turn now to the impact on forecasts. To what extent does the additional assimilation of altimeter data impact the forecasts? To answer this, four extensive sets of coupled model forecasts were intercompared. The results show that the rmse of the forecasts initialized from the combined assimilation of sea level and temperature data is comparable to that of forecasts that use only temperature data. This is only one measure of skill, however, and if one adopts other methods of assessment, there are hints that the forecasts using altimeter and temperature data and the correction of salinity based on the preservation of the T–S relationship, have higher correlation in the Niño-3 region. Tests using hit and false alarm statistics and relative performance statistics also suggest improvement for this set of forecasts, especially at longer lead times.

The inclusion of altimetry leads to smaller improvement in forecast skill than we had hoped. Two caveats need to be borne in mind, however. It is likely that model error is a major contributor to forecast error. The same coupled model is used for all the experiments. If model error dominates, then improvements in the creation of

initial conditions will not be allowed to show a proper impact on the forecasts. A second consideration is that basically the same OI scheme is used throughout for assimilating in situ data. If the decorrelation scales or other parameters or procedures of the OI are badly chosen then again the potential impact of adding altimetry will be reduced. Other experiments at ECMWF suggest that while the TAO array does a very good job of constraining the thermal structure when using the decorrelation scales used in this paper, there is emerging evidence that these scales are too large. If they were reduced then the altimeter might again have more impact than seen in this work.

Finally one might hope that the assimilation of sea level observations would improve the forecasts in the tropical Atlantic and Indian Oceans, where few direct temperature observations exist. However, it is not clear to what extent the forecast skill in these areas depends on the local subsurface temperature structure. For the equatorial Pacific there is evidence for such a connection, but for the Atlantic and Indian Oceans such dependence may be weak in most cases. We have not examined the SST forecasts in this region in detail but it appears that both predictability and skill are limited.

*Acknowledgments.* This work has been supported by the European Union Environment and Climate project DUACS (ENV4-CT96-0357) and the Centre National d'Etudes Spatiales (CNES). The altimeter products have been produced by the CLS Space Oceanography Division as part of the European Union Environment and Climate Project AGORA (ENV4-CT9560113) and DUACS (ENV4-CT96-0357). The ocean model was provided by the Max-Planck-Institut für Meteorologie, Hamburg, Germany; ocean data assimilation software by the Bureau of Meteorology Research Centre, Melbourne, Australia; and coupling software by CERFACS, Toulouse, France.

#### REFERENCES

- Carton, J. A., B. S. Giese, X. Cao, and L. Miller, 1996: Impact of altimeter, thermistor and expendable bathythermograph data on retrospective analyses of the tropical Pacific Ocean. *J. Geophys. Res.*, **101**, 14 147–14 159.
- , G. Chepurin, X. Cao, and B. Giese, 2000: A simple ocean data analysis of the upper ocean, 1950–95. Part I: Methodology. *J. Phys. Oceanogr.*, **30**, 294–309.
- Cooper, M., and K. Haines, 1996: Altimetric assimilation with water property conservation. *J. Geophys. Res.*, **101**, 1059–1077.
- Daley, R., 1991: *Atmospheric Data Analysis*. Cambridge University Press, 457 pp.
- Derber, J., and A. Rosati, 1989: A global data assimilation system. *J. Phys. Oceanogr.*, **19**, 1333–1347.
- Fischer, M., M. Flügel, M. Ji, and M. Latif, 1997: The Impact of data assimilation on ENSO simulations and predictions. *Mon. Wea. Rev.*, **125**, 819–829.
- Gill, A. E., 1979: *Atmosphere–Ocean Dynamics*. Academic Press, 662 pp.
- Ji, M., D. W. Behringer, and A. Leetma, 1998: An improved coupled model for ENSO prediction and implications for ocean initialization. Part II: The coupled model. *Mon. Wea. Rev.*, **126**, 1022–1034.
- , R. W. Reynolds, and D. W. Behringer, 2000: Use of TOPEX/POSEIDON sea level data for ocean analyses and ENSO prediction: Some early results. *J. Climate*, **13**, 216–231.
- Kessler, W. S., 1999: Interannual variability of the subsurface high salinity tongue south of the equator at 165°E. *J. Phys. Oceanogr.*, **29**, 2038–2049.
- Le Traon, P. Y., P. Gaspar, F. Bouyssel, and H. Makhmara, 1995: Using TOPEX/POSEIDON data to enhance ERS-1 orbit. *J. Atmos. Oceanic Technol.*, **12**, 161–170.
- , F. Nadal, and N. Ducet, 1998: An improved mapping method of multi-satellite altimeter data. *J. Atmos. Oceanic Technol.*, **15**, 522–534.
- Levitus, S., and T. Boyer, 1994: Temperature. Vol. 4, *World Ocean Atlas 1994*, NOAA Atlas NESDIS, 117 pp.
- , R. Burgett, and T. P. Boyer, 1994: Salinity. Vol. 3, *World Ocean Atlas 1994*, NOAA Atlas NESDIS, 99 pp.
- Masina, S., N. Pinardi, and A. Navarra, 2000: A global ocean temperature and altimeter data assimilation system for studies of climate variability. *Climate Dyn.*, **17**, 687–700.
- Mellor, G. L., and T. Ezer, 1991: A Gulf Stream model and an altimeter assimilation scheme. *J. Geophys. Res.*, **96**, 8779–8795.
- Meyers, G., H. Phillips, N. Smith, and J. Sprintall, 1991: Space and time scales for optimal interpolation of temperature—Tropical Pacific Ocean. *Progress in Oceanography*, Vol. 28, Pergamon, 189–218.
- Palmer, T., and D. L. T. Anderson, 1994: Prospects for seasonal forecasting. *Quart. J. Roy. Meteor. Soc.*, **120**, 755–794.
- Reynolds, R. W., and T. M. Smith, 1995: A high resolution global sea surface temperature climatology. *J. Climate*, **8**, 1 571–1 583.
- Schopf, P. S., and M. J. Suarez, 1988: Vacillations in a coupled ocean–atmosphere model. *J. Atmos. Sci.*, **45**, 549–566.
- Segsneider, J., D. L. T. Anderson, and T. N. Stockdale, 2000a: Toward the use of altimetry for operational seasonal forecasting. *J. Climate*, **13**, 3116–3138.
- , M. Balmaseda, and D. L. T. Anderson, 2000b: Anomalous hydrographic variations in the tropical Atlantic: possible causes and implications for the use of altimeter data. *Geophys. Res. Lett.*, **27**, 2281–2284.
- Smith, N. R., J. E. Blomley, and G. Meyers, 1991: A univariate statistical interpolation scheme for subsurface thermal analyses in the tropical oceans. *Progress in Oceanography*, Vol. 28, Pergamon, 219–256.
- Stockdale, T. N., 1997: Coupled ocean–atmosphere forecasts in the presence of climate drift. *Mon. Wea. Rev.*, **125**, 809–818.
- Troccoli, A., and K. Haines, 1999: Use of the temperature salinity relation in a temperature assimilation context. *J. Atmos. Oceanic Technol.*, **16**, 2011–2025.
- , M. Balmaseda, J. Segsneider, J. Vialard, D. L. T. Anderson, K. Haines, T. N. Stockdale, and F. Vitart 2001: Salinity adjustments in the presence of temperature data assimilation. *Mon. Wea. Rev.*, in press. [Also available online as ECMWF Tech. Memo. 305, at [www.ecmwf.int](http://www.ecmwf.int).]
- Vossepel, F. C., R. W. Reynolds, and L. Miller, 1999: Use of sea level observations to estimate salinity variability in the tropical Pacific. *J. Atmos. Oceanic Technol.*, **16**, 1401–1415.
- Weaver, A., and J. Vialard, 1999: Development of an ocean incremental 4D-Var scheme for seasonal prediction. *Proc. Third WMO Int. Symp. on Assimilation of Observations in Meteorology and Oceanography*, Quebec City, QC, Canada, WMO, 191–194.
- Wolff, J. O., E. Maier-Reimer, and S. Legutke, 1997: The Hamburg Ocean Primitive Equation Model. Deutsches Klimarechenzentrum Tech. Rep. 13, Hamburg, Germany, 98 pp.
- Zebiak, S. E., 1993: Air–sea interaction in the equatorial Atlantic region. *J. Climate*, **6**, 1567–1586.